ISSN 1024-8560, Atmospheric and Oceanic Optics, 2015, Vol. 28, No. 4, pp. 381–386. © Pleiades Publishing, Ltd., 2015.
Original Russian Text © A.L. Rukosuev, A.V. Kudryashov, A.N. Lylova, V.V. Samarkin, Yu.V. Sheldakova, 2015, published in Optika Atmosfery i Okeana.

ADAPTIVE AND INTEGRAL OPTICS

Adaptive Optics System for Real-Time Wavefront Correction

A. L. Rukosuev, A. V. Kudryashov, A. N. Lylova, V. V. Samarkin, and Yu. V. Sheldakova

Moscow State University Mechanical Engineering (MAMI), ul. Bol'shaya Semenovskaya 28, Moscow, 107023 Russia
e-mail: alru@nightn.ru, kud@activeoptics.ru, ann_lylova@activeoptics.ru, samarkin@activeoptics.ru, sheldakova@nightn.ru

Received November 6, 2014

Abstract—A rapid adaptive system for atmospheric turbulence compensation is considered in the work. It operates with a frequency of 200 Hz. A deformable mirror with 97 piezoactuators as a stacked actuator and a 2-kHz Shack–Hartmann wavefront sensor have been used for the adaptive system design. A dependence of the residual error of a sine signal correction on the speed of system response is also considered.

Keywords: adaptive optics, deformable mirror, atmospheric turbulence, Shack–Hartmann wavefront sensor

DOI: 10.1134/S1024856015040119

Data communication through the Earth's atmosphere with an optical signal is currently an object of multiple studies [1]. Long-distance wireless transport of energy or information along both vertical and horizontal light beam paths is an example. Optical systems have some advantages, such as a possibility of widening a frequency band available for signal transfer and interception security.

However, one should remember that radiation propagating in the atmosphere to long distances is strongly affected by atmospheric turbulence, which distorts the wavefront; along with light diffraction, this results in loss of signal quality and a decrease in the signal power density [2]. Hence, improvement of the reliability of operation of optical systems under different weather conditions is required. The use of adaptive optics techniques and elements, in particular, radiation wavefront correctors, is one of the most promising ways of solution of the above problem. A wavefront corrector is capable of compensating signal distortions caused by turbulent fluctuations in the Earth's atmosphere via real-time variations in its profile [3].

It is of particular interest to consider the process of dynamic correction of aberrations. A closed adaptive optics system (AOS) is discrete in time, since wavefront data arrive from a video camera in the form of individual frames with a certain clock speed. Hence, if a correction algorithm does not use an extrapolation method, then the arriving signal is also discrete in time, and the frequency of variation in this signal does not exceed the wavefront sensor camera framerate.

Any real signal is a continuous function; therefore, system operation with the use of a time-discrete sample inevitably results in an error caused by the fact that the executive element (wavefront corrector) remains invariable in a span between control signals, while the input signal changes. In a real system, the correction error is even a little higher, because a control signal is fed to the adaptive mirror not at the instant of wavefront measurement, but with a delay due to input data processing [4].

It is convenient to consider the process of discrete correction using a sinusoidal input signal as an example. This process in shown in Fig. 1 for the case of the proportional algorithm. It is assumed that an ideal adaptive system first measures an input signal and then produces a correcting signal equal to the input signal but reversed in sign. When producing the control signal, only the time delay equal to the sample period (video camera framerate) is considered. Other time delays or correction errors are ignored. The correction is evidently lacking when using 10 samples per sinusoid period (see Fig. 1a); however, a decrease in the input signal amplitude by about two times is possible at 30 samples per period (Fig. 1b). The results are more or less acceptable when about 100 correction samples fall into a sinusoid period (see Fig. 1c). In this case, the residual correction error is 0.1 of the input signal amplitude.

Figure 2 shows a typical AOS that can affect the wavefront.

An input laser beam falls to a key AOS element (deformable mirror, DM) and then reflects toward the receiver (target). A translucent beam splitter branches a part of the DM-reflected laser beam to a wavefront sensor (WFS). Data from the WFS are input into a computer; using a certain algorithm, the computer calculates the control voltages that should be applied to the DM to correct the incident radiation wavefront. A DM control unit amplifies the voltages calculated to a value required for normal operation of the DM.

The choice of system elements is determined by the problems that should be solved with the system. Thus, if radiation propagates along an inclined path 2–3 km long

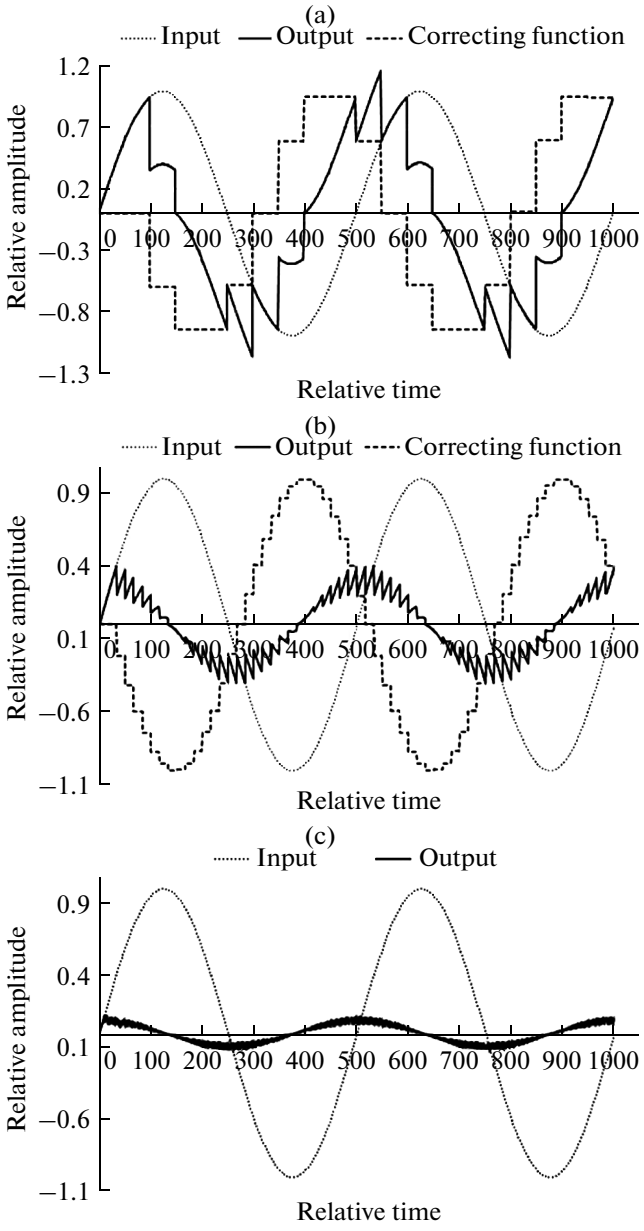

Fig. 1. Correction results at (a) 10, (b) 30, and (c) 100 measurements per period.

at an angle of 45°, the characteristic frequencies of atmospheric turbulence phase fluctuations on the aperture D of 400 mm are about 70 Hz [5]. Moreover, atmospheric turbulence usually generates small-scale wavefront distortions, which have a characteristic size of about 40 mm at a wavelength $\lambda \sim 500$ nm in this case. Thus, the ratio of the aperture diameter to the coherence length is equal to 10; hence, it is reasonable to choose a DM with pushers (stacked-actuators) among all flexible mirrors or effective compensation of such distortions. Such a mirror has the following advantages:

1) quick response to the control voltage applied;

2) local response functions, which allows correcting small-scale wavefront fluctuations;

3) sufficiently wide dynamic range of variations in the mirror surface curvature.

Other types of controllable mirrors are not completely appropriate for solution of the problem of atmospheric turbulence correction. For example, bimorph mirrors operate very rapidly, but have modal response functions, which does not allow their use for compensation of small-scale fluctuations [6–8]. Mirrors based on microelectromechanical systems are currently very expensive, unreliable in service, and insufficiently rapid [9].

Figure 3 shows the general view of a mirror and interferograms of response functions of individual piezomotor drives.

Specifications of the corrector designed are given below.

Active aperture	50 mm
Piezomotor drive size	2 × 3 × 12 mm
Working voltage range	−100 to +300 V
Space between piezomotor drives	4.5–5.0 mm
Arrangement configuration of piezomotor drives	square, 11 × 11
Number of piezomotor drives	97
Maximal deflection	±3.5 μm
Frequency of the first resonance of piezomotor drives	15 kHz
Optical coating	Ag
Weight	920 g

It is reasonable to use a Shack–Hartmann sensor as a WFS for solution of the problem stated [10–12]. Among its advantages are the following:

1) capability of rapid wavefront analysis;

2) low sensitivity to variations in the radiation intensity and to vibrations;

3) easy-to-use;

4) relatively low cost.

According to the principle of operation of the sensor, the wavefront is divided into individual segments, within which the local tilt is considered constant. Depending on the phase front tilt, focal spots formed by a microlens dot pattern are displaced. These displacements are proportional to local tilts of the wavefront, and, hence, the radiation wavefront structure can be retrieved from measurements of tilt values.

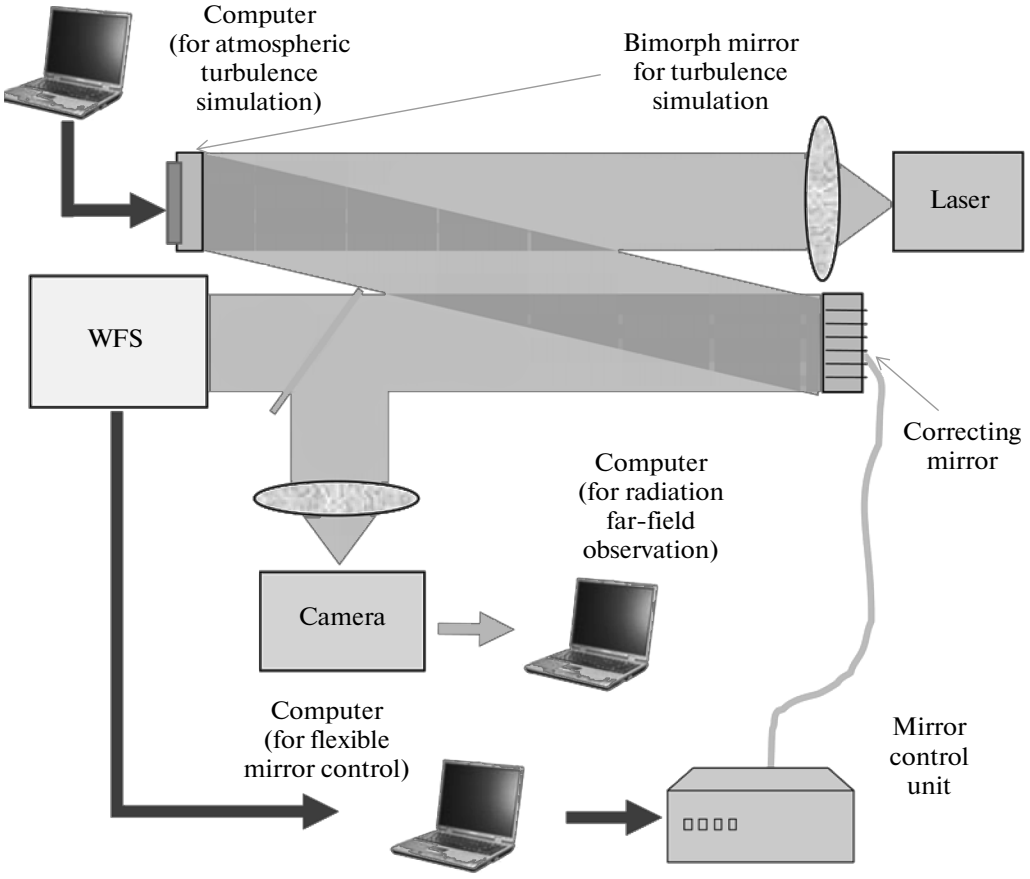

Fig. 2. Experimental setup.

In particular, the radiation wavefront can be retrieved using the modal method for phase derivative expansion in Zernicke polynomials [13]:

$$\frac{\partial\varphi(x_k,y_k)}{\partial x}=\sum_{p=1}^{NP}a_p\frac{\partial Z_p(x_k,y_k)}{\partial x}$$
$$\text{and}\ \ \frac{\partial\varphi(x_k,y_k)}{\partial y}=\sum_{p=1}^{NP}a_p\frac{\partial Z_p(x_k,y_k)}{\partial y}, \qquad (1)$$

where NP is the number of expansion polynomials; a_p are the expansion coefficients at Zernicke polynomials; $Z_p(x_k, y_k)$ are the values of a Zernicke polynomial of the pth order at points (x_k, y_k). Since the local tilts are proportional to displacements of the focal spots ΔS, one may write

$$\frac{\Delta\varphi}{\Delta x}=\frac{1}{f}S_x^k,\ \ \frac{\Delta\varphi}{\Delta y}=\frac{1}{f}S_y^k \qquad (2)$$

(f is the microlens focus). The set of equations derived can be represented in matrix form as $S = adZ$, where S is the vector of displacements with respect to the focus f; a are the coefficients in the Zernicke polynomials; dZ is the rectangular matrix of derivatives of 2D Zernicke polynomials of $NP \times 2NK$ in size (NK is the number of spots on a hartmannogram).

When choosing a camera for the WFS, the main requirements are for the camera speed. We used a Pho-

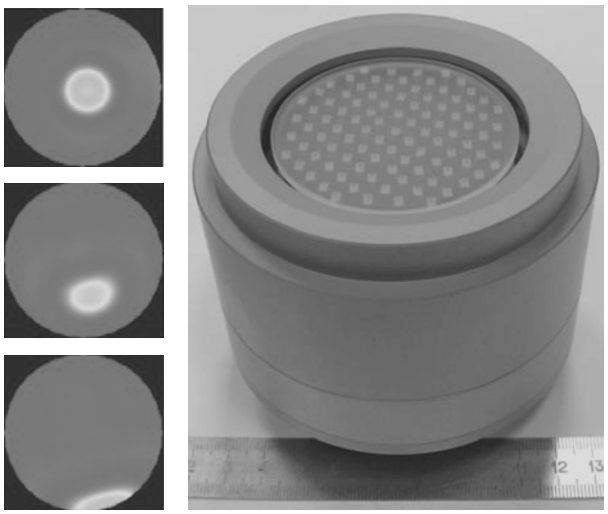

Fig. 3. General view of the adjustable mirror and response functions of individual drives.

ton Focus CMOS camera MV-D752-160-CL-8. Having a high speed, of up to 2 kHz at an image size of 256 × 256 pixels, it can be used in an adaptive system. An image from the camera is transmitted to a computer through the Camera Link digital interface, which requires a corresponding extension board in the computer, e.g., a photoinput of the Camera Link microEnable III standard.

Another element, determining the choice of a Shack–Hartmann sensor, is a microlens dot pattern. Microlens size and the focal length should agree with both the camera sensor size and the step of control drives, their number, and aberrations which are to be measured. Considering all the requirements, a microlens dot pattern with a rectangular arrangement of the lenses of 160 × 160 μm in size and a focal length of 6 mm was chosen.

Main specifications of the Shack–Hartmann sensor are given below.

Working wavelength range	350–1100 nm
Spatial resolution	160 μm
Measurement accuracy	wavelength/100
Frequency of data acquisition and processing	up to 1000 Hz
Computer interface	Camera Link
Focal length of lens dot pattern	6 mm
Number of working subapertures	16 × 16
Input beam size	2.5 × 2.5 mm
Sensor sizes	62 × 54 × 68 mm
Weight	300 g

There are several approaches to control the voltage at DM electrodes. The phase conjugation approach is the best for implementation of the rapid correction. The essence of the approach consists in the following: the DM surface takes such a form under which the wavefront of a surface-reflected laser beam corresponds to the required wavefront. A plane wavefront at the adaptive system exit is required the most often.

A Shack–Hartmann WFS is a difference device; therefore, an input beam is analyzed relative to a certain initial arrangement of the focal spots of the lens dot pattern. A set of coordinates of the focal spot centers that answer the initial position is called the reference. During the wavefront correction by the phase conjugation method, DM voltages are calculated so as the coordinates of the focal points after the beam has been corrected maximally approach the reference coordinates after application of the correcting voltages [14]. These voltages can be calculated with, e.g., the mean-square method. Let us represent the magnitudes of displacements of the focal points of the lens pattern as the matrix

$$S_i = \begin{vmatrix} \Delta x_i \\ \Delta y_i \end{vmatrix} = \sum_{j=1}^{N} u_j b_j^i, \quad (3)$$

where N is the number of mirror electrodes; u are the mirror electrode voltages; b are the elements of the DM response function. The mirror electrode response function is a set of coordinates of focal spot displacements in response for a voltage of unit amplitude applied to the electrode:

$$b_{jx}^i = \Delta x_i / u_{0j}, \quad (4)$$

$$b_{jy}^i = \Delta y_i / u_{0j}. \quad (5)$$

Here Δx and Δy are the displacements of the focal spots along the corresponding axes; u_0 is the voltage at which the response function changes.

To find a set of mirror electrode voltages by the mean-square method, it is necessary to minimize the functional

$$\min \|\mathbf{S} - b \cdot \mathbf{u}\|^2. \quad (6)$$

The solution is to be found in the form

$$\mathbf{u} = \|\mathbf{B}\| \cdot \mathbf{S}, \quad (7)$$

where

$$B = (b^{\mathrm{T}} b)^{-1} b^{\mathrm{T}} \ (b^{\mathrm{T}} \text{ is the transposed matrix } b). \quad (8)$$

The procedure of wavefront correction in a real AOS is carried our in the following order.

1. Equipment test.

2. Input of the reference array of focal spot coordinates.

3. Measurement of the response function.

4. Wavefront correction:

a) analysis of the wavefront;

b) calculation of control voltages;

c) application of the control voltages to mirror electrodes.

The wavefront correction (item 4) may be performed repeatedly and in real time. To estimate the system speed, time intervals of all the components of item 4 are to be analyzed.

Operation of a WFS is characterized by three time segments: camera exposure time, data transmission from the camera to a computer, and time for focal spot coordinate calculation. In the WFS used, the time required for exposure and data transmission was about 0.5 ms, and the calculation of focal spot coordinates took about 3 ms. Voltage calculations required 1 ms, and the time of main mirror transitions exceeded 0.5 ms. Thus, one correction cycle lasted about 5 ms, which is indicative of a correction frequency of 200 Hz being attained. However, an adaptive system does not allow the wavefront to be completely corrected for one

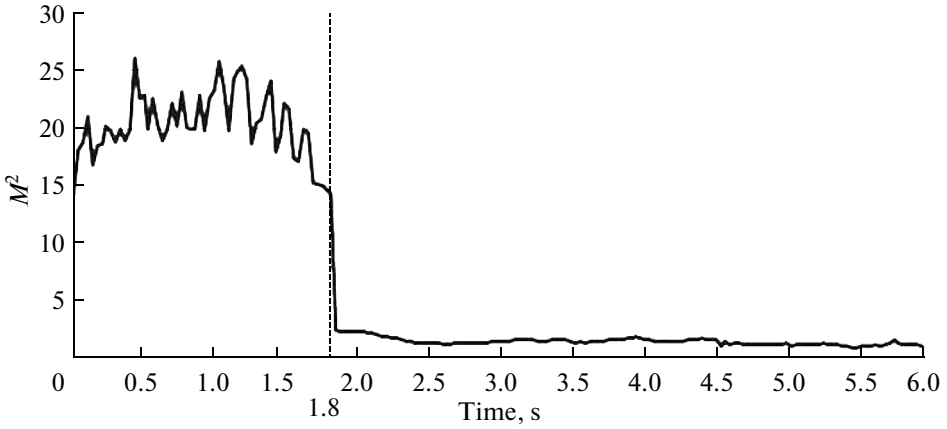

Fig. 4. Time dependence of the parameter M^2 of a laser beam passed through the turbulence generator. The adaptive system was switched on at a time point of 1.8 s.

step (cycle), due to inaccurate measurements of the wavefront, noise, incorrect measurements of the response functions of control elements, etc. Two–three iterations were required for optimal correction in our case; therefore, the closed adaptive system actually operated with a frequency of 65–70 Hz.

The efficiency of turbulent phase fluctuations was studied in the experimental setup (see Fig. 2).

A beam emitted by a photodiode laser is transformed into a parallel one with the use of a convex lens and then comes to the mirror-generator of artificial turbulence. A bimorph flexible mirror with 32 electrodes was used as a turbulence generator [15]; it was controlled through a special algorithm, which reproduces phase screens with a Kolmogorov spectrum in real time [16, 17].

Then the aberrated beam is incident on the correcting DM with pushers, was reflected from it, fell on the WFS, and then through the beam splitter to an independent system for controlling the far-field laser beam intensity (see Fig. 3). A long-focus lens and a JAI CCD array had the following parameters: the sensor size was 1/2″, the resolution, 1392 × 1040, the operating frequency, 30 Hz, the pixel size, 4.65 μm, and a GigE interface.

The measurement results of intensity distribution before and after the correction are shown in Fig. 4.

The turbulence generator introduced large-scale wavefront aberrations starting from the initial time to 1.8 s ($D/r_0 = 6$, r_0 is the Fried's radius; the Greenwood frequency $f_g = 60$); this caused intensity fluctuations at the lens focus which corresponded to the parameter $M^2 = 25 \pm 5$. The M^2 value decreased significantly down to 1.3–1.5 after switching on the adaptive system. Thus, the AOS designed operating with a frequency of up to 200 Hz is capable of correcting the incident radiation wavefront with a frequency of 65–70 Hz. The correction results were confirmed by independent measurements of the far-field intensity distribution.

It is clear that the experiment cannot fully show the capabilities of the wavefront correction system designed. However, the results hold out a hope for the efficient use of similar systems in real conditions for aberration compensation of light signals passing through atmospheric layers.

REFERENCES

1. F. Yu. Kanev and V. P. Lukin, *Adaptive Optics. Numerical and Experimental Researches* (Publishing House of IAO SB RAS, Tomsk, 2005) [in Russian].
2. V. A. Banakh and I. N. Smalikho, "Laser beam propagation along extended vertical and slant paths in the turbulent atmosphere," Atmos. Ocean. Opt. **6** (4), 233–237 (1993).
3. A. V. Kudryashov and V. I. Shmalhausen, "Semipassive bimorph flexible mirror for atmospheric adaptive optics applications," Opt. Eng. **35** (11), 3064–3073 (1996).
4. F. Yu. Kanev, V. P. Lukin, and L. N. Lavrinova, "Dynamic adaptive mirror in the algorithm of phase conjugation," Atmos. Ocean. Opt. **8** (12), 1061–1064 (1995).
5. A. K. Gupta and S. K. Mishra, "Development of adaptive optics imaging system at IRDE," in *Proc. XXXV OSI Symposium, International Conference on Contemporary Trends in Optics and Opto Electronics, January, 17–19, 2011* (Thiruvananthapuram, India, 2011), pp. 19–21.
6. V. Samarkin, A. Aleksandrov, and A. Kudryashov, "Bimorph mirrors for powerful laser beam correction and formation," in Proc. SPIE. **4493**, 269–276 (2002).
7. A. Rukosuev, A. Alexandrov, V. Zavalova, V. Samarkin, and A. Kudryashov, "Adaptive optical system based on bimorph mirror and Shack–Hartmann wavefront sensor," Proc. SPIE **4493**, 261–268 (2002).
8. A. Kudryashov, V. Samarkin, and A. Aleksandrov, "Adaptive optical elements for laser beam control," Proc. SPIE **4457**, 170–178 (2001).

9. P. Bierden, T. Bifano, and S. Cornelissen, "MEMS deformable mirrors for high performance AO applications," *Proc. of the 6th Int. Workshop "Adaptive Optics for Industry and Medicine,"* Ed. by Christopher Dainty (National University of Ireland, Ireland, 2007), pp. 65–70.
10. F. Yu. Kanev, V. P. Lukin, B. V. Fortes, and P. A. Konyaev, "Numerical model of an atmospheric adaptive optical system. II. Wave-front sensors and control elements," Atmos. Ocean. Opt. **8** (3), 215–219 (1995).
11. A. G. Aleksandrov, V. E. Zavalova, A. V. Kudryashov, A. L. Rukosuev, Yu. V. Sheldakova, V. V. Samarkin, and P. N. Romanov, "Shack–Hartmann wavefront sensor for measuring the parameters of high-power pulsed solid-state lasers," Quantum Electron. **40** (4) 321–327 (2010).
12. Y. Akahane, J. Ma, Y. Fukuda, M. Aoyoma, H. Kiriyama, K. Yamakawa, J. V. Sheldakova, and A. V. Kudryashov, "Characterization of wave-front corrected 100 tW, 10 Hz laser pulses with peak intensities greater than 1020 w/cm^2," Rev. Sci. Instrum. **77** (2), 023102-1–023102-7 (2006).
13. J. V. Sheldakova, A. V. Kudryashov, V. Y. Zavalova, and T. Y. Cherezova, "Beam quality measurements with Shack–Hartmann wavefront sensor and m2-sensor: Comparison of two methods," Proc. SPIE **6452**, 645207 (2007).
14. A. V. Kudryashov, V. V. Samarkin, Yu. V. Sheldakova, and A. G. Aleksandrov, "Wavefront compensation method using a Shack–Hartmann sensor as an adaptive optical element system," Optoelectron., Instrum. Data Proc. **48** (2), 153–158 (2012).
15. V. Samarkin and A. Kudryashov, "Deformable mirrors for laser beam shaping," Proc. SPIE **7789**, 77890B (2010).
16. A. Lylova and A. Kudryashov, "Artificial model of human eye aberrations proceeded in real-time," in *Abstracts of the 9th International Workshop on Adaptive Optics for Industry and Medicine AOIM2013, September 2–6, 2013, Stellenbosch, South Africa,* p. 30.
17. D. C. Dayton, S. L. Brown, S. P. Sandven, J. D. Gonglewski, and A. V. Kudryashov, "Theory and laboratory demonstration on the use of a nematic liquid crystal phase modulator for controlled turbulence generation and adaptive optics," Appl. Opt. **37** (24), 5579–5589 (1998).

Translated by O. Ponomareva